Meccanica (2019) 54:1403–1419
https://doi.org/10.1007/s11012-019-01019-x

Parameters identification of cable stayed footbridges using Bayesian inference

Chiara Pepi · Massimiliano Gioffre' · Mircea D. Grigoriu

Received: 14 February 2019 / Accepted: 4 July 2019 / Published online: 17 July 2019

Abstract Numerical modeling of actual structural systems is a very complex task mainly due to the lack of complete knowledge on the involved parameters. Simplified assumptions on the uncertain geometry, material properties and boundary conditions make the numerical model response differ from the actual structural response. Improvements of the finite element (FE) models to obtain accurate response predictions can be achieved by vibration based FE model updating which uses experimental measures to minimize the differences between the numerical and experimental modal features (i.e. natural frequencies and mode shapes). Within this context, probabilistic model updating procedures based on the Bayes' theorem were recently proposed in the literature in order to take into account the uncertainties affecting the structural parameters and their influence on the structural response. In this paper, a novel framework to efficiently estimate the posterior marginal PDF of the selected model parameters is proposed. First, the main dynamic parameters to be used for model updating are identified by ambient vibration tests on an actual structural system. Second, a first numerical FE model is developed to perform initial sensitivity analysis. Third, a surrogate model based on polynomial chaos is calibrated on the initial FE model to significantly reduce computational costs. Finally, the posterior marginal PDFs of the chosen model parameters are estimated. The effectiveness of the proposed method is demonstrated using a FE numerical model describing a curved cable-stayed footbridge located in Terni (Umbria Region, Central Italy).

Keywords Cable-stayed footbridge · Finite element model · Operational modal analysis · Surrogate model · Polynomial chaos expansion · Global sensitivity analysis · Bayesian inference

C. Pepi (✉) · M. Gioffre'
CRIACIV/Department of Civil and Environmental Engineering, University of Perugia, via G. Duranti 93, 06125 Perugia, Italy
e-mail: chiara.pepi@unipg.it

M. Gioffre'
e-mail: massimiliano.gioffre@unipg.it

M. D. Grigoriu
Department of Civil and Environmental Engineering, Cornell University, 220 Hollister Hall, Ithaca, NY 14853, USA
e-mail: mdg12@cornell.edu

1 Introduction

Cable-stayed footbridges and bridges are gaining worldwide interest because of some inherent features that determine the reduction of deck bending moments and deformations under live loads when compared to suspension bridges [20]. Despite the aforementioned advantages against the suspended layout, cable-stayed

bridges and footbridges still pose serious concerns regarding the high sensitivity to dynamic loads, mainly pedestrian and wind action, affecting the structural performance of the structure.

Within this context, the development of reliable and accurate structural FE models is of utmost importance to accurately predict the bridge response to different dynamic loading conditions. Therefore, the careful assessment of the system modal characteristics in operating conditions using experimental tests becomes crucial to develop a suitable FE model updating technique [13].

The commonly used approach consists of determining the structural parameters (mainly the structural members stiffness) which minimize the differences between the modal properties computed with the FE model and those estimated from experimental data recorded on the actual structure [23]. Ambient vibration tests (AVT) can be used to obtain these data given the assumption of linear structural behavior under low amplitude loads [7, 8, 15, 16, 32, 33]. Response time histories are recorded under the assumption of stationary white noise loads and the obtained data can be processed using operational modal analysis (OMA) algorithms in the frequency and/or time domain [10, 12, 29, 31].

Beside classical deterministic approaches, in the last few years probabilistic model updating procedures have gained growing interest in the scientific community since they are able to take into account the uncertainties affecting the FE model parameters and their influence on the structural response [22]. A review of the probabilistic approach can be found in [27, 37] and [42]. This kind of techniques can be grouped in two main classes: classical probabilistic approaches and Bayesian methods based on the well known Bayes' theorem [4].

A complete Bayesian framework relies on the knowledge of the prior uncertain parameters probability density functions (PDFs) and takes explicitly into account all the sources of uncertainties involved in the process, including measurement and modeling uncertainies, to obtain updated probability estimates for the random parameters in terms of joint, or marginal, PDFs and/or confidence intervals [5, 6, 46]. In the Bayesian updating procedure a complex multidimensional integration problem has to be solved that can be rather time consuming especially when several updating parameters are modified during the process and/or when a large data set is used as reference [30]. The Markov Chain Monte Carlo (MCMC) methods are the most widely used techniques for such integration and are based on the generation of random sequences of input parameters samples (so called Markov chains) that are in equilibrium with the target posterior PDFs [19, 24]. These methods require several solutions of the structural problem using the deterministic FE model, one for each occurrence of the input parameters, that can make the Bayesian procedure unfeasible.

Surrogate models based on PC expansion [26, 41] can be used to solve this issue, dramatically reducing the time needed for the Bayesian updating framework by replacing the numerical FE model solution with the surrogate solution. PC expansions are generally used in stochastic finite element (SFEM) to describe the random model response by a set of coefficients in a suitable PC basis [21, 44, 45]. The number of terms to be computed increases with the number of input random variables (RVs) making the computational effort with sampling based methods unpractical. A non intrusive regression method based on the deterministic evaluations of the FE model solution in a few number of points can be used to address this problem [14].

Once the surrogate models are calibrated, they can also be used to carry out efficient global sensitivity analysis (GSA) based on the model output variance decomposition method [35, 38, 39]. GSA aims to quantify the effect of the random input parameters on the model output variance. The PC expansions method gives the opportunity to evaluate the sensitivity indices analytically, starting from the PC coefficients, without adding computational costs. An accurate GSA is a crucial point in the Bayesian updating framework since gives the chance to reduce the model order, neglecting all the structural elements not affecting the uncertainty analysis results.

In this paper, a novel approach to overcome the main limitations of the commonly used Bayesian framework in efficiently updating a numerical model when incomplete experimental dynamic modal data are available is proposed. First, estimates of the modal parameters are obtained via AVTs on an actual structural system. Second, sensitivity analysis is performed to select the structural parameters that have significant influence on the system natural frequencies. Third surrogate models are calibrated on the initial FE model and a GSA is performed to have more

information on the uncertain parameters influence on the selected modal features. Finally, a modified version of the MCMC method is used to estimate the posterior marginal PDF of the selected model parameters: (a) beside the commonly used system natural frequencies, the modal assurance criterion (MAC) is used to ensure direct mode shape matching at each step of the chain; (b) the deterministic FE model solution is replaced with the PC surrogate solution at each evaluation step in order to dramatically reduce the computational costs required to estimate the posterior marginal PDFs. The effectiveness of the proposed method is eventually demonstrated using a FE numerical model describing a curved cable-stayed footbridge located in Terni (Umbria Region, Central Italy).

2 Bayesian inference for inverse problems

In recent years structural and modal identification have been addressed using the Bayesian updating framework to estimate FE model parameter from measured dynamic data [2, 6]. This approach is based on the Bayesian interpretation of probability which differs from the frequentist one. In the latter, probability is viewed as the relative occurrence of a random phenomena, whereas in the Bayesian interpretation, probability is seen as the plausibility of a hypothesis. Within this context the structural parameters uncertainty is given by the incomplete availability of information/data.

2.1 Uncertainty quantification framework

Consider a numerical mechanical model $\mathcal{M}$ characterized by an input random vector $\boldsymbol{\Theta} = \{\Theta_1, \ldots, \Theta_n\} \in \mathbb{R}^n$ consisting in n independent random parameters defined according to some probability space $\{\Omega, \mathcal{F}, \mathcal{P}\}$ where Ω is the probability space, $\mathcal{F}$ is the σ-field and $\mathcal{P}$ is the probability measure.

If each Θ_i, $i = 1, 2, \ldots, n$, is described by the probability density function $\pi_i(\theta_i)$, the joint PDF is given by the product of the n densities. Let the relation between the vector $\boldsymbol{\Theta}$ and the associated output response quantities $\mathbf{u} = \{u_1, \ldots, u_m\} \in \mathbb{R}^m$ given by the forward problem $\mathcal{M}$

$$\mathbf{u} = \mathcal{M}(\boldsymbol{\Theta}) \tag{1}$$

with $\mathcal{M} : \mathbb{R}^n \rightarrow \mathbb{R}^m$. The output response $\mathbf{u}$ represents the quantity of interest (QoI) of the uncertainty quantification (UQ) problem.

If system modal characteristics are of interest, two different kind of uncertainties, that affect both experimental and numerical predictions, have to be properly taken into account: measurement and model uncertainties. The most obvious source of uncertainty comes from the recorded data. Measurements errors determine a difference between the observed structural behavior $\overline{\mathbf{D}} = \{\overline{d}_1, \ldots, \overline{d}_m\} \in \mathbb{R}^m$ and the actual response $\mathbf{D} = \{d_1, \ldots, d_m\} \in \mathbb{R}^m$. For this reason measurements uncertainties are taken into account defining the modal prediction error

$$\overline{\boldsymbol{\epsilon}} = \overline{\mathbf{D}} - \mathbf{D} \tag{2}$$

Model uncertainties are due to lack of knowledge on the actual mechanical and geometrical properties, materials, boundary conditions, construction process and type of coupling between the structural components. These uncertainties are considered defining the model prediction error

$$\boldsymbol{\epsilon} = \mathbf{D} - \mathcal{M}(\boldsymbol{\Theta}) \tag{3}$$

that gives information on the difference between the actual structural behavior $\mathbf{D}$ and the numerical model prediction vector $\mathcal{M}(\boldsymbol{\Theta})$.

Both modal and model prediction errors need to be considered in order to improve the matching between the numerical model and the data estimations. The total error is the difference between the model predictions and the observed quantities (i.e. estimated from data) and can be obtained by Eqs. (2) and (3)

$$\overline{\boldsymbol{\epsilon}} + \boldsymbol{\epsilon} = \overline{\mathbf{D}} - \mathcal{M}(\boldsymbol{\Theta}) \tag{4}$$

which represents the main equation for the whole UQ problem, avoiding to explicitly consider the unknown actual structural response $\mathbf{D}$.

2.2 Bayes' theorem

In the Bayesian approach, the probabilities of the unknown parameters Θ_i, $i = 1, 2, \ldots, n$, characterizing a model class M when new data $\overline{\mathbf{D}}$ becomes available is given by the joint PDF

$$p(\boldsymbol{\Theta}|\overline{\mathbf{D}}, M) = c^{-1} p(\overline{\mathbf{D}}|\boldsymbol{\Theta}, M) p(\boldsymbol{\Theta}|M) \tag{5}$$

which is known as *posterior distribution*.

The term $p(\overline{\mathbf{D}}|\boldsymbol{\Theta}, M)$, called *likelihood function*, expresses the joint probability of the data, conditional to the unknown/adjustable vector $\boldsymbol{\Theta}$, and the model class M. The term $p(\boldsymbol{\Theta}|M)$ is the *prior distribution*, which quantifies the initial plausibility of the vector of parameters $\boldsymbol{\Theta}$ associated with the model class M. The normalizing constant $c = p(\overline{\mathbf{D}}|M)$, called the *evidence of model class M*, makes the integration of the posterior PDF in (5) over the parameter space equal to one. The c constant can be estimated by the multidimensional integration over the parameter space

$$c = p(\overline{\mathbf{D}}|M) = \int p(\overline{\mathbf{D}}|\boldsymbol{\Theta}) p(\boldsymbol{\Theta}|M) d\boldsymbol{\Theta} \tag{6}$$

In the following, the explicit dependence on the model class M will be omitted since a single FE model only will be considered.

2.2.1 Prior PDF

The prior PDF, $p(\boldsymbol{\Theta})$, describes the probability of the FE model parameters when no evidence/information are taken into account. A very general classification of the Bayesian prior probabilities can be made according to the way they are selected, distinguishing between subjective and objective priors. The subjective priors are chosen depending on expert judgment, i.e. personal belief. This subjective choice can be relevant since different results of the Bayesian updating framework may be obtained when the data set used as reference is small or not properly informative. On the contrary, objective priors are formulated according to some formal rules like the widely used principle of maximum entropy [25].

2.2.2 Likelihood function

The likelihood function $p(\overline{\mathbf{D}}|\boldsymbol{\Theta})$ can be interpreted as a measure of the accuracy of the model in describing the measurements. The likelihood function can be obtained according to the total probability theorem as the convolution of the measurement and modeling errors PDFs [3, 36]

$$p(\overline{\mathbf{D}}|\boldsymbol{\Theta}) = \int p_{\overline{\mathbf{e}}}(\overline{\mathbf{D}} - \mathbf{D}|\boldsymbol{\Theta}, \overline{\mathbf{D}}) p_{\mathbf{e}}(\mathbf{D} - \mathcal{M}(\boldsymbol{\Theta})|\boldsymbol{\Theta}) d\mathbf{D} \tag{7}$$

where $p_{\overline{\mathbf{e}}}(\mathbf{D} - \overline{\mathbf{D}}|\boldsymbol{\Theta}, \overline{\mathbf{D}})$ is the joint probability of the measurement error $\overline{\mathbf{e}}$ when the model is driven by a set of parameters $\boldsymbol{\Theta}$ and the selected data set $\overline{\mathbf{D}}$, while $p_{\mathbf{e}}(\mathbf{D} - \mathcal{M}(\boldsymbol{\Theta})|\boldsymbol{\Theta})$ is the probability of obtaining the modeling error $\mathbf{e}$ given the same set of parameters $\boldsymbol{\Theta}$.

When no information is available on the individual errors, the likelihood function can be formulated modeling the total prediction error in (4) as a Gaussian vector with zero mean and a constant unknown variance σ^2 for all the components, making the likelihood function in (7) a M-variate joint PDF:

$$p(\overline{\mathbf{D}}|\boldsymbol{\Theta}) \propto exp\left(-\frac{1}{2} (\overline{\mathbf{e}} + \mathbf{e})^T \boldsymbol{\Sigma}^{-1} (\overline{\mathbf{e}} + \mathbf{e}) \right) \tag{8}$$

where $\boldsymbol{\Sigma}$ is the $[m \times m]$ total error covariance matrix.

2.2.3 Posterior PDF

Once the prior PDF and the likelihood function are defined, experimental observations and Eq. (5) are used to obtain the marginal posterior PDFs of the updating parameters Θ_i. If the number of parameters and the data space dimension is large, the multidimensional integration in (5) cannot be solved with analytical approaches. Most of the estimates are commonly computed with deterministic (quadrature or cubature) or sampling based (Monte Carlo or Lathyn Hypercube) numerical methods.

Markov Chain Monte Carlo (MCMC) is the most recent and widely used procedure for posterior sampling [19]. The term MCMC refers to all the procedures that are based on random sequences of samples (so called Markov Chain) which are in equilibrium with the target posterior PDF, i.e. that are subject to some acceptance criteria. Each step of the procedure depends on the previous steps. It follows that the PDF can be estimated by targeting a posterior PDF without knowing the scaling factor c in Eq. (6).

Metropolis Hastings (MH) is the most known MCMC method [24]. It requires the computation of the forward problem in (1) at each step of the chain and it requires about 10^5 sample generations to have solution convergency. This approach can be computationally prohibitive.

3 Spectral expansion for Bayesian updating

In order to obtain a significant reduction of the computational burden for the evaluation of the Bayesian integral in Eq. (5) described in the previous section, an effective method is proposed in this section. The main idea is to use the well known PC expansion [21], decomposing the forward model response in Eq. (1) into polynomial terms that are orthogonal with respect to a weighting function identified as a probability density. The combined use of both these surrogate models and the MAC coefficients as soft constraint in computing the likelihood function represent the main novelty of the proposed framework.

3.1 Polynomial chaos representation

Let $\boldsymbol{\Theta} \in \mathbb{R}^n$ be a non Gaussian random vector with n independent components defined by

$$\boldsymbol{\Theta} = \mathbf{g}(\boldsymbol{\xi}) \tag{9}$$

where $\mathbf{g}$ is a nonlinear function, $\mathbf{g} : \mathbb{R}^k \rightarrow \mathbb{R}^n$, $\boldsymbol{\xi} \sim N(0, \boldsymbol{I})$ is a $\mathbb{R}^k$-valued vector of k independent and identically distributed, zero mean, unit variance Gaussian random variables (RVs) and $\mathbf{I}$ denotes the identity matrix with dimensions $(k \times k)$. The solution of the physical model in (1) can be written as

$$\mathbf{u} = \mathcal{G}(\boldsymbol{\xi}) \tag{10}$$

where $\mathcal{G} : \mathbb{R}^k \rightarrow \mathbb{R}^m$.

Considering a k-variate model input and a univariate model output, i.e. $m = 1$, and assuming that the model response is a finite variance RV, the PC representation of the structural response can be written as

$$u = \sum_{\boldsymbol{\alpha} \in \mathbb{N}^k} \hat{\boldsymbol{u}}_{\boldsymbol{\alpha}} \boldsymbol{\Psi}_{\boldsymbol{\alpha}}(\boldsymbol{\xi}) \tag{11}$$

where $\boldsymbol{\Psi}_{\boldsymbol{\alpha}}(\boldsymbol{\xi})$ represents the multivariate Hermite polynomials with finite multi-index set and $\hat{\boldsymbol{u}}_{\boldsymbol{\alpha}}$, $\boldsymbol{\alpha} \in \mathbb{N}^k$, are the polynomial coefficients. The set of multivariate polynomials in the input random vector $\boldsymbol{\xi}$ is orthogonal with respect to the Gaussian measure.

3.2 Polynomial chaos approximation

The representation in Eq. (11) describes the random system response exactly when an infinite series is considered. In practice, an appropriate truncation scheme needs to be developed.

Considering the k-dimensional polynomials of order not exceeding p, the response u in (11) may be approximated using

$$\tilde{u} = \tilde{\mathcal{G}}(\boldsymbol{\xi}) = \sum_{\boldsymbol{\alpha} \geq 0}^{N_p - 1} \hat{\boldsymbol{u}}_{\boldsymbol{\alpha}} \boldsymbol{\Psi}_{\boldsymbol{\alpha}}(\boldsymbol{\xi}) \tag{12}$$

where $\tilde{\mathcal{G}}(\boldsymbol{\xi})$ represents the surrogate model. In this case, the number of unknown (vector) coefficients in the summation is given by

$$N_p = \binom{k+p}{p} = \frac{(k+p)!}{k!p!} \tag{13}$$

The polynomial order has to be chosen to guarantee results accuracy. As an example, in stochastic finite element model (SFEM) applications it is common to choose p between 3 and 5. A suitable convergence analysis can be carried out to determine the optimal PC expansion order [9, 26].

The PC expansion was initially formulated using standard Gaussian random input parameters and Hermite polynomials [44] but it is in general possible to model input system parameters with any non-Gaussian distribution using suitable mapping with isoprobabilistic transformations. However, it is worth noting some limitations of PC expansion: the rate of convergence of the PC approximation may be slow; accuracy improvements can not be achieved even if adding terms; moments higher than two calculated form PC approximation can be not accurate; PC approximations for stationary non-Gaussian stochastic processes might not be stationary [17].

3.3 Computation of the deterministic coefficients

The deterministic coefficients $\hat{\boldsymbol{u}}_{\boldsymbol{\alpha}}$ in (12) can be computed using different approaches: stochastic Galerkin, orthogonal projection and regression [28]. The stochastic Galerkin method is classified as intrusive since the deterministic solver has to be modified in order to obtain the stochastic solution. Alternatively, non intrusive methods based on the deterministic solutions of the input realizations have been recently proposed.

The non intrusive regression method presented in [14] is used in this work and it is based on the

minimization of the mean square error in the response approximation. To this aim, the random response of the model is written as

$$\mathcal{G}(\boldsymbol{\xi}) = \tilde{\mathcal{G}}(\boldsymbol{\xi}) + \varepsilon = \sum_{\boldsymbol{\alpha} \geq 0}^{N_P - 1} \hat{\boldsymbol{u}}_{\boldsymbol{\alpha}} \boldsymbol{\Psi}_{\boldsymbol{\alpha}}(\boldsymbol{\xi}) + \varepsilon \tag{14}$$

where the residual error ε collects the truncated PC terms. The regression approach consists in finding the set of coefficients $\hat{\boldsymbol{u}} = \{\hat{u}_{\boldsymbol{0}}, \ldots, \hat{u}_{N_p - \boldsymbol{1}}\}^T$ which minimizes the variance of the residual error

$$\hat{\boldsymbol{u}} = arg \quad min \left\{ \mathbb{E}\left[\left(\mathcal{G}(\boldsymbol{\xi}) - \sum_{\boldsymbol{\alpha} \geq 0}^{N_P - 1} \hat{\boldsymbol{u}}_{\boldsymbol{\alpha}} \boldsymbol{\Psi}_{\boldsymbol{\alpha}}(\boldsymbol{\xi}) \right)^2 \right] \right\} \tag{15}$$

i.e. the best approximation of the mathematical model $\mathcal{G}(\boldsymbol{\xi})$. The discretized version of the continuous problem in (15) is based on a set of $N_R > N_P$ regression points gathered in the vector $\mathcal{X} = \{\boldsymbol{\xi}^{\boldsymbol{1}}, \ldots, \boldsymbol{\xi}^{\boldsymbol{N_R}}\}$, called experimental design (ED). For each of these points a set of N_R realizations of the input vector $\boldsymbol{\Theta}$ can be evaluated according to Eq. 9.

The least square minimization problem can therefore be solved by minimizing the mean square truncation error

$$\hat{\boldsymbol{u}} = arg \quad min \frac{1}{N_R} \sum_{i=1}^{N_R} \left\{ \mathcal{G}(\boldsymbol{\xi}^i) - \sum_{\boldsymbol{\alpha} \geq 0}^{N_P - 1} \hat{\boldsymbol{u}}_{\boldsymbol{\alpha}} \boldsymbol{\Psi}_{\boldsymbol{\alpha}}(\boldsymbol{\xi}^i) \right\}^2 \tag{16}$$

where $\mathcal{U} = \{\mathcal{G}(\boldsymbol{\xi}^{\boldsymbol{1}}), \ldots, \mathcal{G}(\boldsymbol{\xi}^{\boldsymbol{N_R}})\}$ is the vector collecting the numerical model responses at the selected regression points. Equation (16) is equivalent to the linear system

$$\hat{\boldsymbol{u}} = (\mathcal{A}^T \mathcal{A})^{-1} \mathcal{A}^T \mathcal{U} \tag{17}$$

where $\mathcal{A}$ is the Vandermonde like design matrix defined as

$$\mathcal{A} = \begin{bmatrix} \psi_0(\boldsymbol{\xi}^{\boldsymbol{1}}) & \psi_1(\boldsymbol{\xi}^{\boldsymbol{1}}) & \cdots & \psi_{N_P-1}(\boldsymbol{\xi}^{\boldsymbol{1}}) \\ \psi_0(\boldsymbol{\xi}^{\boldsymbol{2}}) & \psi_1(\boldsymbol{\xi}^{\boldsymbol{2}}) & \cdots & \psi_{N_P-1}(\boldsymbol{\xi}^{\boldsymbol{2}}) \\ \vdots & \vdots & \ddots & \vdots \\ \psi_0(\boldsymbol{\xi}^{\boldsymbol{N_R}}) & \psi_1(\boldsymbol{\xi}^{\boldsymbol{N_R}}) & \cdots & \psi_{N_P-1}(\boldsymbol{\xi}^{\boldsymbol{N_R}}) \end{bmatrix} \tag{18}$$

that needs to be not singular in order to have a well defined problem, i.e. $\mathcal{A}^T\mathcal{A}$ has to be positive definite and invertible.

The number of regression points should be larger than the number of the unknown PC coefficients to ensure the numerical stability of the regression points. It is worth noting that the choice of the regression points highly influence the accuracy of the results. One possible choice is to generate these sampling points using the Gaussian quadrature rule with a full tensor grid scheme evaluating the deterministic solution at $(p+1)^n$ sampling points [41].

3.4 Moment analysis

Given the orthogonality conditions of the PC expansion basis the output response statistics can be estimated from the deterministic coefficients. In particular, the mean value $\mu_{\tilde{u}}$ and the variance $\sigma^2_{\tilde{u}}$ of the surrogate model response $\tilde{u}$ can be obtained by

$$\mu_{\tilde{u}} = \mathbb{E}[\tilde{\mathcal{G}}(\boldsymbol{\xi})] = \mathbb{E}\left[\sum_{\boldsymbol{\alpha} \geq 0}^{N_P - 1} \hat{\boldsymbol{u}}_{\boldsymbol{\alpha}} \boldsymbol{\Psi}_{\boldsymbol{\alpha}}(\boldsymbol{\xi}) \right] = \hat{u}_0 \tag{19}$$

$$\sigma^2_{\tilde{u}} = \mathbb{E}[(\tilde{\mathcal{G}}(\boldsymbol{\xi}) - \hat{u}_0)^2] = \sum_{\boldsymbol{\alpha} \neq 0} \hat{\boldsymbol{u}}_{\boldsymbol{\alpha}}{}^2 \tag{20}$$

where $\boldsymbol{\Psi}_{\boldsymbol{0}} = 1$ and $\mathbb{E}[\boldsymbol{\Psi}_{\boldsymbol{\alpha}}(\boldsymbol{\xi})] = 0, \forall \boldsymbol{\alpha} \neq 0$.

3.5 Global sensitivity analysis

The influence of the input parameters on the output QoI can be quantified using sensitivity analysis. Input factors are considered unessential when they have no effect on the output variability. The identification of unessential input parameters can lead to significant reduction of the problem dimension. This aspect is crucial especially when dealing with probabilistic design problems or Bayesian updating for the estimation of input parameters.

Within this context, the global sensitivity analysis (GSA) method is one of the most widely used and it is based on the variance decomposition of the random system output as [38, 39]

$$\mathrm{Var}[\mathcal{M}(\boldsymbol{\Theta})] = \sum_{i=1}^{n} V_i + \sum_{i<j}^{n} V_{i,j} + \cdots + V_{1,2,\ldots,n} \tag{21}$$

where

$$V_i = \mathrm{Var}_{\Theta_i}(\mathbb{E}_{\Theta_{\tilde{i}}}[\mathcal{M}(\boldsymbol{\Theta})|\Theta_i]) \tag{22}$$

$$V_{ij} = \mathrm{Var}_{\Theta_{ij}}(\mathbb{E}_{\Theta_{\tilde{ij}}}[\mathcal{M}(\boldsymbol{\Theta})|\Theta_i, \Theta_j]) - V_i - V_j \tag{23}$$

with $i,j = 1,\ldots,n$ and $\Theta_{\tilde{i}}$ indicates the set of all parameters except Θ_i. The total variance of the model output is thus decomposed into a sum of terms depending on each input random parameter taken alone and on their interactions.

If all terms in Eq. 21 are divided by $\mathrm{Var}[\mathcal{M}(\boldsymbol{\Theta})]$ one obtains

$$1 = \sum_{i=1}^{N} S_i + \sum_{i<j}^{N} S_{i,j} + \cdots + S_{1,2,\ldots,N} \tag{24}$$

where S_i and $S_{i,j}$ are the so-called Sobol' indices. The first order indexes S_i quantify the influence of each single random parameter on the response variance and can be computed directly by

$$S_i = \frac{Var[V_i]}{Var[\mathcal{M}(\boldsymbol{\Theta})]} \tag{25}$$

while the higher order indexes $S_{i,j}$ quantify the influence of all possible combination of the input random parameters on the response variance and are given by

$$S_{i,j} = \frac{Var[V_{ij}]}{Var[\mathcal{M}(\boldsymbol{\Theta})]} \tag{26}$$

Once that PC coefficients are defined, the Sobol' indices can be easily evaluated as a function of the deterministic coefficients [40], significantly reducing the computational cost if compared to sampling based method, e.g. Monte Carlo or Quasi Monte Carlo.

3.6 Posterior evaluation based on polynomial chaos expansion

Once the PC expansion coefficients are obtained, the surrogate model can be used to obtain a response surface $u(\boldsymbol{\xi})$ analytically (Eq. (10)) and to perform the posterior sampling via MCMC avoiding the time consuming solutions of the numerical model $\mathcal{M}(\boldsymbol{\Theta})$.

A suitable choice of the operator $\mathbf{g}$ in Eq. (9) becomes crucial depending on the chosen PC basis and the polynomial order. Indeed, errors due to the functional approximation of the surrogate model responses may cause fallacious results of the Bayesian updating framework. For this reason, one has to carefully validate the surrogate model in order to obtain significant results. With this approach, the likelihood function in (8) can be computed using an indirect method based on a surrogate solution of the forward model and the posterior marginal distributions are estimated using samples of $\boldsymbol{\xi}$.

The updating process can cause misleading results when experimental modal data are used as reference because of possible frequency matching associated to different mode shapes. To overcome this problem the main idea is to use the MAC coefficient [1] in order to measure the correlation rate between the experimental and numerical mode shapes. MAC coefficient assumes values ranging from 0 to 1, when the two modes have zero or perfect correlation, respectively. The classical MCMC MH algorithm is thus modified using the MAC coefficients as soft constraint so that the total error in Eq. (4) at each step of the chain is computed as the difference between the model predicted and the observed natural frequencies only when they correspond to the same mode shape.

4 Case study

4.1 Initial FE model

The footbridge under investigation in this work is named "Umbria Gateway" and is located in Terni—Umbria Region—100 km north from Rome (Fig. 1). The footbridge has a total length of 180 m and has two main parts: a curved shape one with a total length of 120 m, which is supported by an asymmetric array of cables connected to a 60 m tall inverted tripod tower through a pair of circular rings; a straight 60 m span with two bowstring arches. The footbridge plan view of the curved shape spans is shown in Fig. 2.

A three-dimensional FE model of the cable-stayed spans was built using the software SAP 2000 [34]. The bridge geometry was carefully described and different mechanical characteristics were selected for the structural components (Table 1). Each stay was modeled with a nonlinear element describing both tension-

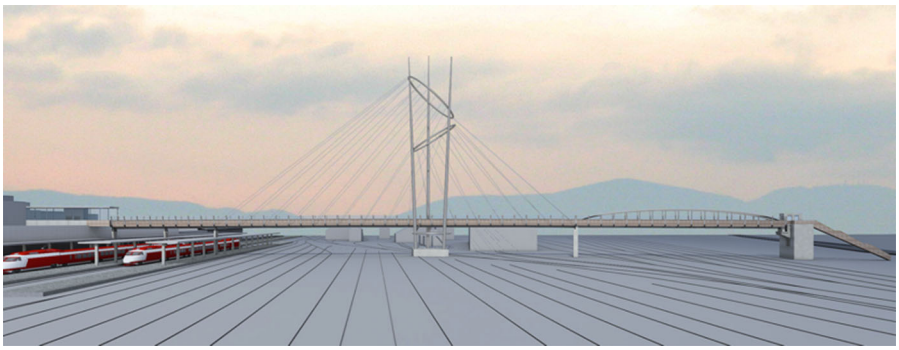

Fig. 1 View of the "Umbria Gateway" cable-stayed footbridge

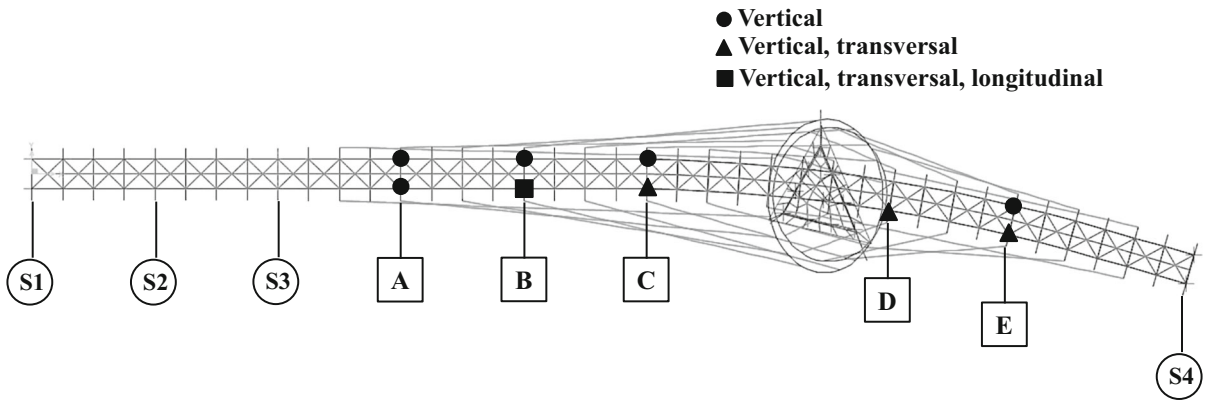

Fig. 2 Plan view and measurement locations on the cable-stayed spans

Table 1 Mechanical properties used in the initial FEM

Material	E (GPa)	Mass density (kN/m^3)
Steel S355	210	78
Cables	160	77
Concrete C32/40	33.345	25

stiffening and large deflections so that an iterative solution is required.

Several authors investigated the significance of the nonlinear behavior of this class of bridges, mainly due to cable sag and large deflection [18, 43]. Cable sag is usually the most significant feature since cable stiffness becomes larger when cable tension increases. For this reason, the dynamic characteristics were estimated performing two types of modal analysis: ordinary modal analysis (MA 1) in the undeformed equilibrium configuration; pre-stress modal analysis (MA 2) in the dead load and cable pre-tension deformed equilibrium configuration. In the latter, large displacements non linear static analysis was performed and the stiffness matrix updated by means of 200 incremental steps. The equilibrium was reached at each step using the iterative Newton–Raphson method.

Table 2 reports the results obtained with the two modal analyses. As expected, the cable pretension cause increased footbridge natural frequencies. Although the differences are very small, the reference deformed configuration is crucial to estimate the dynamic response to wind and/or earthquake loads. Eight mode shape types were found in the range of frequencies of interest 0–3.5 Hz: five are vertical; two are lateral and one is torsional. It is worth noting that some dominant modes have frequencies very close to each other.

4.2 Dynamic identification

The footbridge dynamic characterization in terms of natural frequencies and corresponding vibration mode

Table 2 Modal features obtained from MA 1 and MA 2

Mode	MA 1 (Hz)	MA 2 (Hz)	Difference (%)	Mode's type
1	1.025	1.030	0.49	Vertical
2	1.491	1.514	1.52	Lateral
3	1.766	1.774	0.45	Torsional
4	2.180	2.184	0.18	Vertical
5	2.306	2.365	2.49	Lateral
6	2.977	2.982	0.17	Vertical
7	3.151	3.153	0.06	Vertical
8	3.419	3.423	0.12	Vertical

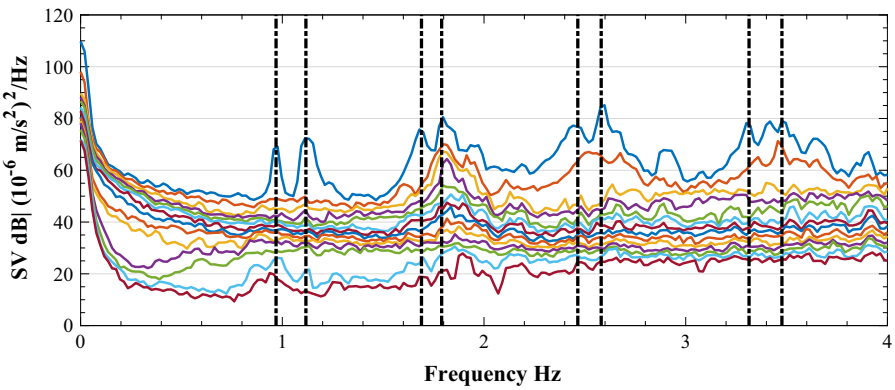

Fig. 3 Non zero singular values plots for data set #2

shapes was obtained from full-scale measurements in operating conditions using classical contact sensors. The dynamic response was recorded using fourteen uni-axial accelerometers (10 V/g sensitivity) located in the five cross-sections A, B, C, D and E of the bridge deck (Fig. 2). The obtained acceleration time histories were used to identify vertical, horizontal and torsional vibration modes with the enhanced frequency domain decomposition (EFDD) method [11].

Two different data sets with 400 Hz sampling rate were recorded with time lengths 710 s (data set #1) and 926 s (data set #2), respectively. Data were downsampled with order of decimation 30 and high-pass filtered in order to remove offsets and drifts. Furthermore, different values of the frequency resolution were considered changing the number of frequency lines in the spectral density spectrum. Reliability of results was investigated using different order of decimation and different type of filters. Plots of non-zero singular values are shown in Fig. 3 for data set #2. Eight modes were clearly identified whose frequencies are highlighted with the vertical dashed lines. Table 3 summarizes the minimum, f_{min}, and the maximum, f_{max}, values of the identified natural frequencies considering both data sets #1 and #2, different frequency resolutions and order of decimation 20 and 40. Figure 4 shows the 3D representation of the identified vibration modes. The magnitudes of the mode shapes at sensor locations were identified directly with the measured data, while the other magnitudes were interpolated using the boundary conditions and the identified mode shapes at sensor locations by means of cinematic equations.

Table 3 Range of identified natural frequencies from data sets #1 and #2

Mode	f_{min} (Hz)	f_{max} (Hz)	Mode's type
1	0.97	0.97	Vertical
2	1.11	1.13	Vertical
3	1.67	1.69	Lateral
4	1.79	1.80	Torsional
5	2.40	2.47	Lateral
6	2.58	2.59	Vertical
7	3.30	3.31	Vertical
8	3.35	3.40	Vertical

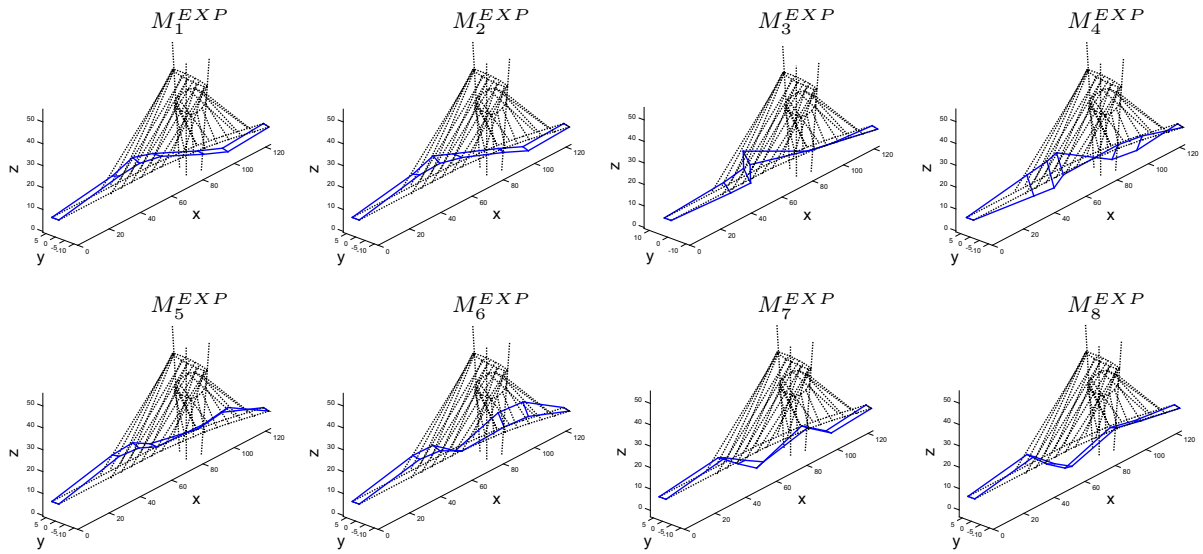

Fig. 4 Vibration modes estimated from experimental data using EFDD

The MAC was used to identify the modal shapes from the experimental data sets. Given a set of modal vectors it is possible to estimate a MAC matrix, whose components are the MAC numbers estimated from each pair of mode shapes. In the following, two different MAC matrices will be estimated: the auto-MAC matrix and the MAC matrix. The first is estimated from the experimental mode shapes while the second is computed pairing one experimental with one numerical mode shape. It is worth noting that the diagonal terms in the auto-MAC matrix are all equal to 1 since each mode shape is paired with itself (Fig. 5a).

The auto-MAC value of the pair given by mode shapes #1 and #2 (bending mode shapes with frequencies below 1.2 Hz) is greater than 0.95. This would indicate that there are high chances that the two vectors describe the same mode shape even if the two corresponding peaks on the singular value curves are clearly separated, being evidence of a sort of mode shape splitting phenomenon. Furthermore, the numerical model presents a single bending mode shape with associated frequency at 1.03 Hz. Further experimental investigation would be needed to assess the actual nature of these identified modes. A possible reason for the observed mode shape splitting could be related to temperature effects and/or high amplitudes of the excitation during the AVTs (e.g. due to wind).

Figure 5b shows the MAC matrix estimated from the experimental mode shapes (data set #2) and the FE analysis. It is worth to note that the higher MAC values are not on the matrix diagonal terms because of the experimental mode shape splitting phenomena described above. These values are greater than 0.80 indicating an initial good correlation between the experimental and numerical modal vectors.

4.3 Deterministic sensitivity analysis and selection of the updating parameters

Selection of the updating parameters is a key issue in the model updating procedure since they have to be directly related to the measurement results used as reference data. This selection usually relies on expert judgment. A preliminary sensitivity analysis was thus carried out in order to have information for an efficient selection. In particular, the sensitivity of the natural frequencies to variations in model mass density, structural steel and cable Young's moduli, cable tension stiffening, stiffness of rotational and translational springs used to describe soil-structure interaction was evaluated.

A first result of the sensitivity analysis is that large variations of both cable tension in each of the stays and spring stiffness, describing the soil-structure interaction, have negligible effects on the numerical model natural frequencies. On the contrary, eigenfrequencies are very sensitive to variations in the steel and cable elasticity moduli, and the model mass density (Fig. 6).

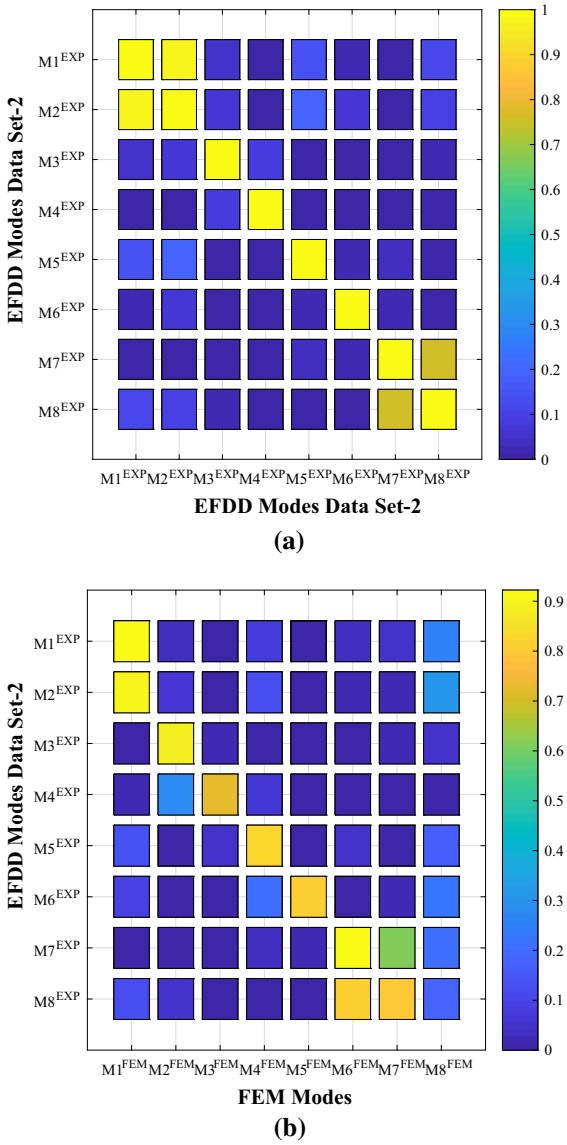

Fig. 5 MAC matrices for data set #2: **a** auto-MAC matrix; **b** MAC matrix

The red star-continuous lines refer to the experimentally identified natural frequencies, while the magenta square-dashed lines refer to the initial numerical model eigenfrequencies. The remaining two lines refer to different choices of the chosen parameters. It is rather clear that it is possible to improve the numerical model if the higher steel moduli and the lower mass density are chosen.

Assuming that the model mass density does not vary significantly along the deck and considering that the Young's modulus and the mass density are correlated, only two updating parameters were selected for the Bayesian framework: the deck and cable stiffnesses described by the steel, E_{steel}, and cable, E_{cables}, elastic moduli, respectively. The real valued random vector $\boldsymbol{\Theta}$ has therefore components $\Theta_1 = E_{steel}$ and $\Theta_2 = E_{cables}$. These random parameters were assumed to be statistically independent.

4.4 Surrogate model validation and global sensitivity analysis

The six natural frequencies, f_i^{EXP}, $i = 2, \ldots, 7$, identified from the experimental data were used as reference, i.e. discarding f_1^{EXP} to account for the possible mode shape splitting described in the previous section. The corresponding six numerical model frequencies f_i^{FEM}, $i = 1, \ldots, 6$, are set as QoIs. The PC expansion in Eq. 12 was used in order to build a surrogate model for each of the selected QoI.

Since no direct information (e.g. measures of the mechanical characteristics) are available for the random vector $\boldsymbol{\Theta}$, a normal distribution was assumed for both components, Θ_1 and Θ_2, to build the six different response surfaces. The mean values of these two PDFs were assumed to be equal to the nominal values of the two different materials used for deck and cables in Table 1, while the coefficient of variations (cov) were set to 0.15 and 0.20 in order to avoid unfeasible samples in the simulation procedure, i.e. the deformed equilibrium configuration with dead load and cables pre-tension was always guaranteed. The resulting two PDFs were used as prior densities in the Bayesian updating.

Each of the six surrogate models was built with a three steps procedure. First, $(p+1)^2$ samples of the input random parameters $\boldsymbol{\Theta}$ were mapped into samples of $\boldsymbol{\xi}$ on a grid selected with the Gaussian quadrature approach using Eq. (9). In this case study $\mathbf{g}$ is a linear function. Second, the deterministic coefficients $\hat{\boldsymbol{u}}_{\boldsymbol{\alpha}}$ in (12) were evaluated using the regression method, which estimates the solution of the numerical model in the regression points and solves the linear system of equations in (15). Third, the difference between the response vectors $\mathbf{u}$ and $\tilde{\mathbf{u}}$, i.e. the error vector, $\tilde{\mathbf{e}}$, was evaluated on the $(p+1)^2$ pairs of samples $\{\theta_1, \theta_2\}$.

The surrogate model was finally validated estimating the mean and the variance of the error vector for polynomial orders, p, equal to 3,4 and 5 (typical of

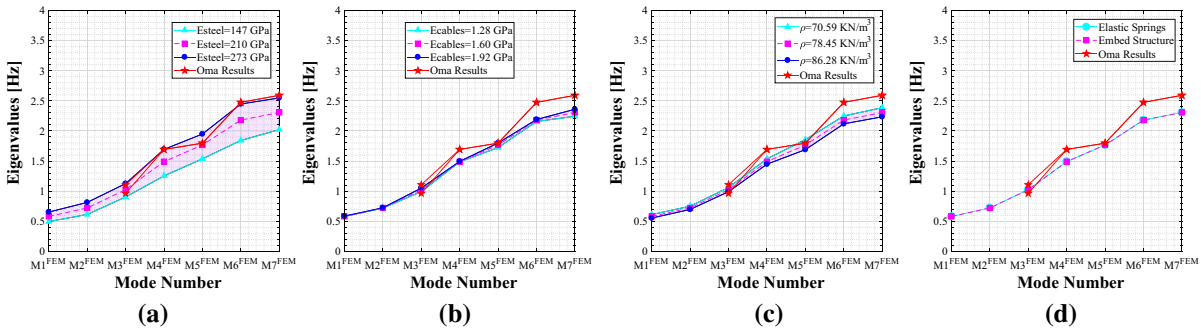

Fig. 6 Eigenfrequencies variations with changes in the mechanical parameters: **a** steel modulus of elasticity; **b** cables modulus of elasticity; **c** model mass density; **d** boundary conditions

SFEM practical applications). Following this procedure it was possible to obtain a perfect matching between numerical and surrogate models with mean and variance of the error vectors lower than 10^{-16} and 10^{-3}, respectively (Fig. 7). It is important to note that the error variance decreases when the polynomial order increases (Fig. 7b), while there is not a clear trend for the error mean (Fig. 7a).

The selection of the best polynomial order was also pursued by estimating the error vector outside the grid used to calibrate the proxy model, driving the simulation of the parameters $\{\theta_1, \theta_2\}$ in the tail values of the vector $\boldsymbol{\Theta}$ joint probability density function. Figure 8 shows the errors, for each of the first six natural frequencies, between the surrogate and the numerical model at two of the tail samples $\{\theta_1, \theta_2\}$, varying the polynomial order. Order $p = 4$ seems to give an accurate solution for all the six proxy models with this selection of the input parameters. Similar plots can be obtained for different selection of the tail values. Polynomial order $p = 5$ was found to be the best selection for all the tested pairs of input parameters.

Figure 9 shows the six surrogate models obtained with polynomial order $p = 5$ in the $\boldsymbol{\xi}$ space, one for each numerical eigenfrequency $\tilde{f}_i^{FEM}$, $i = 1, \ldots, 6.$, together with the corresponding f_i^{EXP} estimated from data (horizontal surface), and the error absolute value, i.e. $|\tilde{f}_i^{FEM}(\boldsymbol{\xi}) - f_i^{EXP}|$ (blue surface).

As it was expected from the sensitivity analyses, the response surfaces show that the natural frequencies are almost constant varying the cable stiffness ξ_2. On the contrary the dependency of the natural frequencies is strongly non linear with the deck stiffness ξ_1.

Once the surrogate models were built, it was possible to estimate the variance of the N_p polynomial coefficients $\hat{\boldsymbol{u}}_{\boldsymbol{\alpha}}$ for each QoI. These variances were used to estimate, for each of the six proxy models, the first and second order Sobol' indices according to Eqs. (25) and (26), which give information on the influence of the uncertain parameters Θ_1, Θ_2 and their combination on the QoI, i.e. the six selected natural frequencies (Fig. 10). The obtained results confirm that the natural frequencies are mainly influenced by the deck stiffness.

4.5 Bayesian inverse problem solution

Setting $\overline{\mathbf{D}} = \{f_2^{EXP}, \ldots, f_7^{EXP}\}$ as reference vector and replacing the numerical model in (10) with the surrogate model (12), the posterior marginal PDF of the two dimensional random vector $\boldsymbol{\Theta} = \{\Theta_1, \Theta_2\}$ can be estimated with Eqs. (5), (6) and (7).

In particular, the MCMC Metropolis Hastings (MH) method was used, sampling directly from the $\boldsymbol{\xi}$ space by replacing the numerical evaluation at each step of the chain with the surrogate solution. The initial covariance matrix of the error in Eq. (8) was assumed to be diagonal with all components equal to 0.01 Hz.

In this work the updating framework was improved using the information given by the diagonal MAC coefficients. In particular, since deck and cables stiffness variations can cause a swap in the natural frequency and mode shapes, the MAC values were used as constraints to guarantee both the natural frequency and mode shape matching at each step of the MH algorithm. Each component of the residual vector $(\overline{\mathbf{e}} + \mathbf{e})$ in Eq. (8) was thus computed as the difference

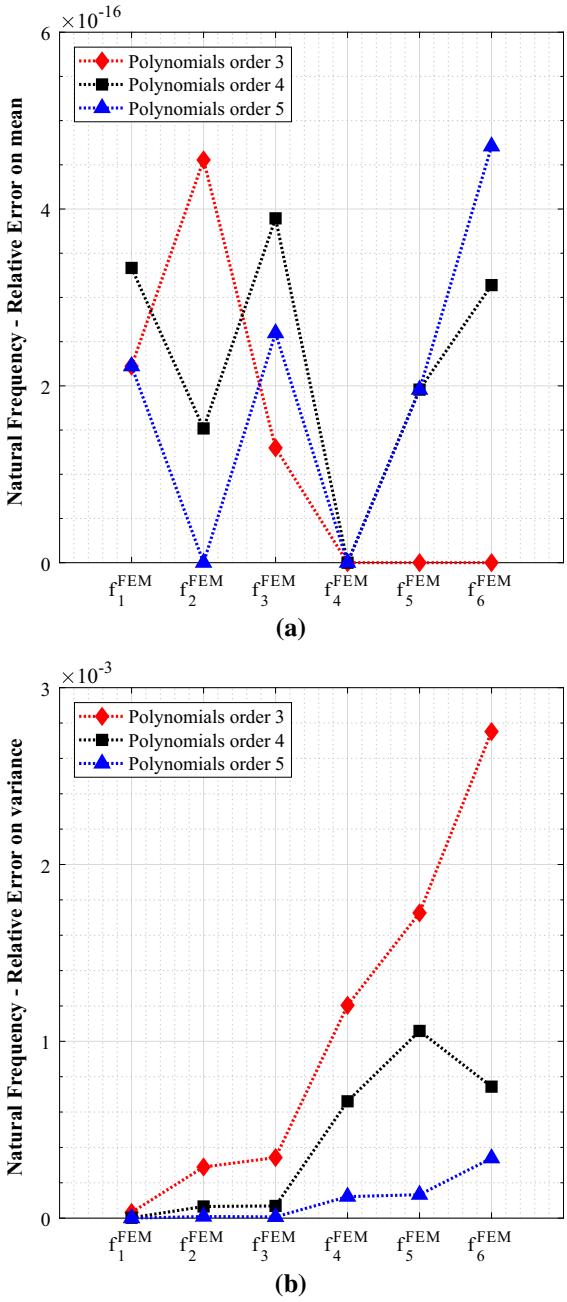

Fig. 7 Variation in the error vectors in the first six natural frequencies for polynomials order 3, 4 and 5: **a** error vector mean; **b** error vector variance

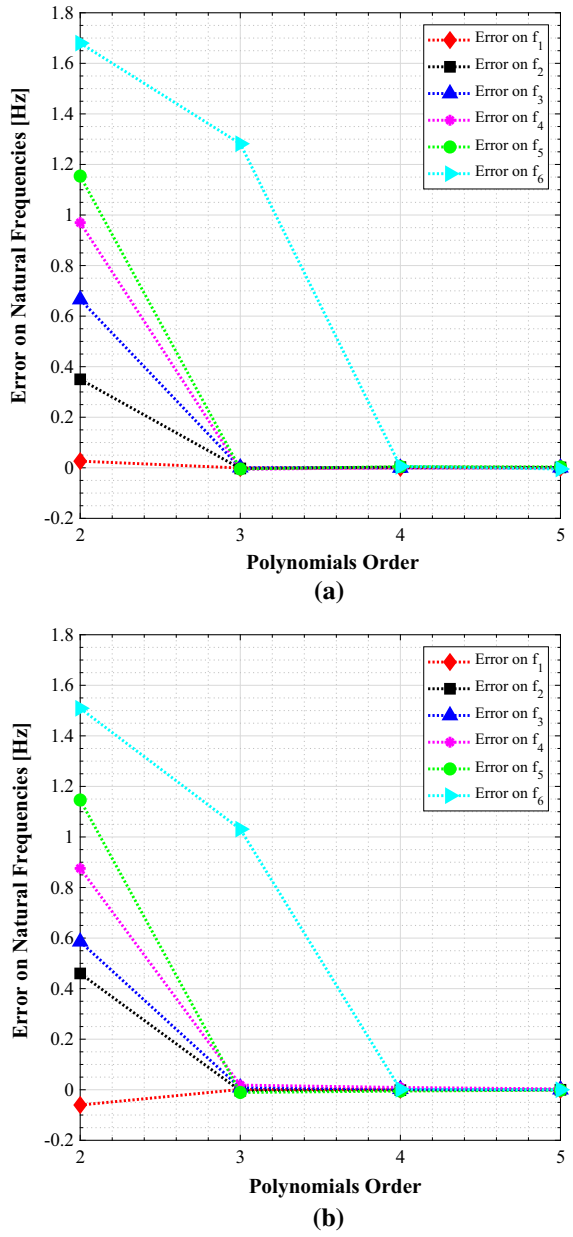

Fig. 8 Difference between the numerical and surrogate first six natural frequencies for polynomials order 3, 4 and 5 for two tail samples of the vector $\boldsymbol{\Theta}$

between the experimental and numerical natural frequencies that have the highest diagonal MAC coefficient.

The modified MCMC MH algorithm was applied generating 40,000 posterior samples that are consistent with the unscaled posterior PDF defined in Sect. 3.6. In order to ensure convergency in this case study, the whole algorithm to estimate the posterior PDF requires the evaluation of the deterministic solution about 150,000 times. If the numerical FE model is used, the updating framework would require more than 5 months since the single analysis

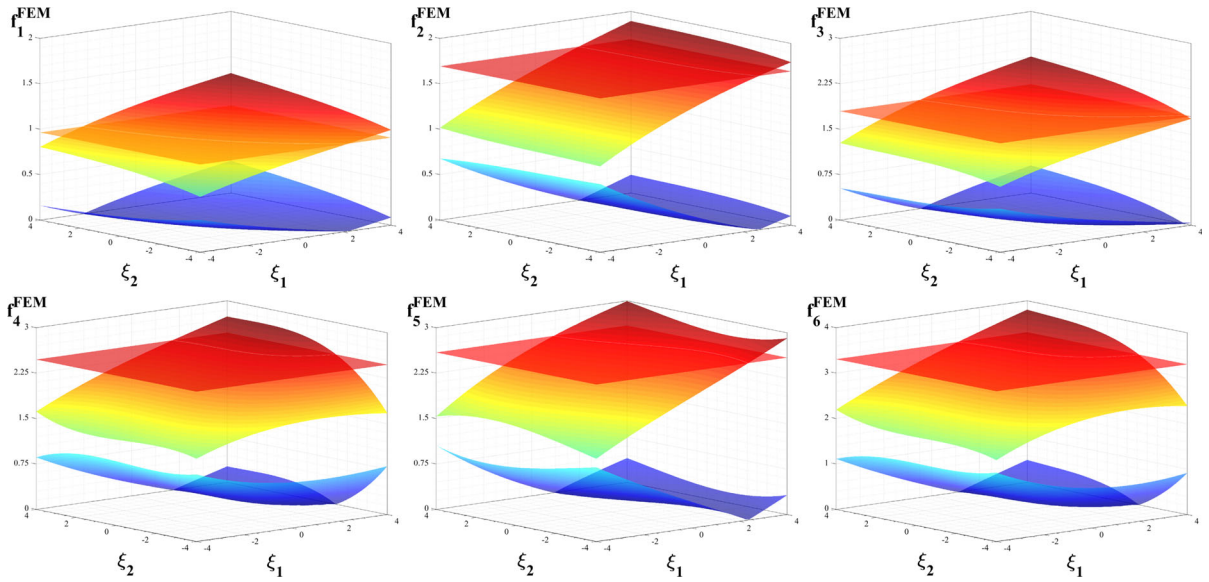

Fig. 9 Surrogate models

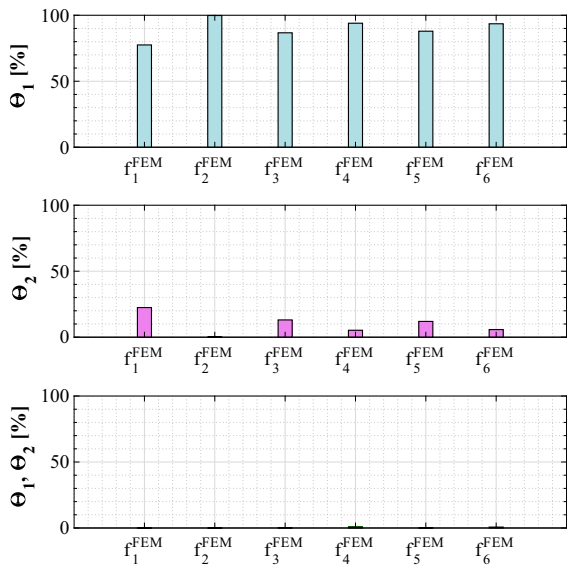

Fig. 10 First and second order Sobol indices for the first six natural frequencies

takes between 1 and 2 min. It is clear that this approach would be unfeasible. The proposed methodology, that uses surrogate models in such a complex cases, makes the solution possible, reducing the computing time to about 60 min.

The results of the proposed updating Bayesian procedure are shown in Figs. 11 and 12. The Θ_1 posterior distribution has mean value equal to 266 GPa, about 1.25 times the mean value of the prior PDF. The Θ_2 posterior distribution is very similar to the prior PDF, indicating that the chosen data set, $\overline{\mathbf{D}}$, is non informative with respect to this random parameter. This result was expected since the natural frequencies are mainly influenced by the deck stiffness, Θ_1, as was shown by the Sobol indices reported in Fig. 10.

Figure 12 shows the response of the FE model before and after the parameters updating. In particular, Fig. 12a compares the experimental natural frequencies with those obtained from the initial and updated numerical model, using the $\boldsymbol{\Theta}$ posterior mean value. The differences between the experimental and the numerical eigenfrequencies before the Bayesian updating procedure were greater than 8%, with the only exception of the 3rd numerical mode shape for which the error was lower than 1%. After the update these errors were reduced to 1%, with the only exception of the 3rd mode shape for which the error is equal to 8%.

Figure 12b compares the MAC values before and after the updating procedure. The initial experimental and numerical mode shapes were characterized by high values of the MAC number (i.e. correlated vectors). After the update the most significant increase of the MAC values, from 73 to 92%, occurs for the 3rd mode shape (torsional). On the contrary the

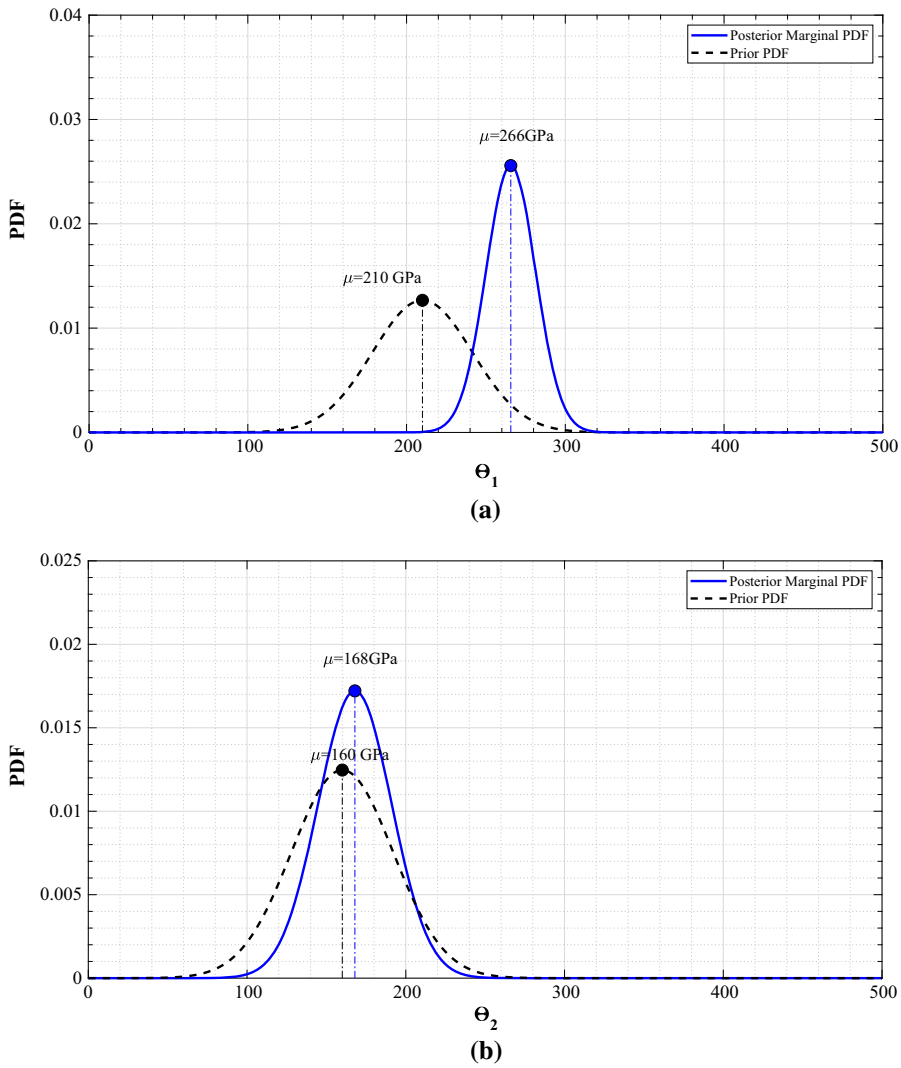

Fig. 11 Prior (dashed line) and posterior (continuous line) distributions: **a** deck stiffness, Θ_1; **b** cable stiffness, Θ_2

diagonal MAC value decreases for the 4th and the 5th mode shape.

5 Conclusion

The work presented in this paper describes a novel approach to overcome the main limitations of the commonly used Bayesian framework in efficiently updating a numerical model when incomplete experimental dynamic modal data are available.

The proposed approach uses in-situ recorded acceleration time histories to estimate natural frequencies and mode shapes by OMA procedures in the frequency domain. A polynomial chaos representation of the dynamic output stochastic response in terms of natural frequencies (i.e. surrogate model) is used both to effectively select the uncertain parameters and to significantly reduce the computation time when estimating the posterior marginal probability density functions by means of a modified MCMC MH procedure.

The main novelty of the proposed approach is given by: (a) the replacement of the FE model response with the surrogate model response; (b) the use of MAC coefficients to ensure direct mode shape matching at each step of the Markov chain.

The effectiveness of the proposed method was demonstrated using a FE numerical model describing a curved cable-stayed footbridge located in Terni

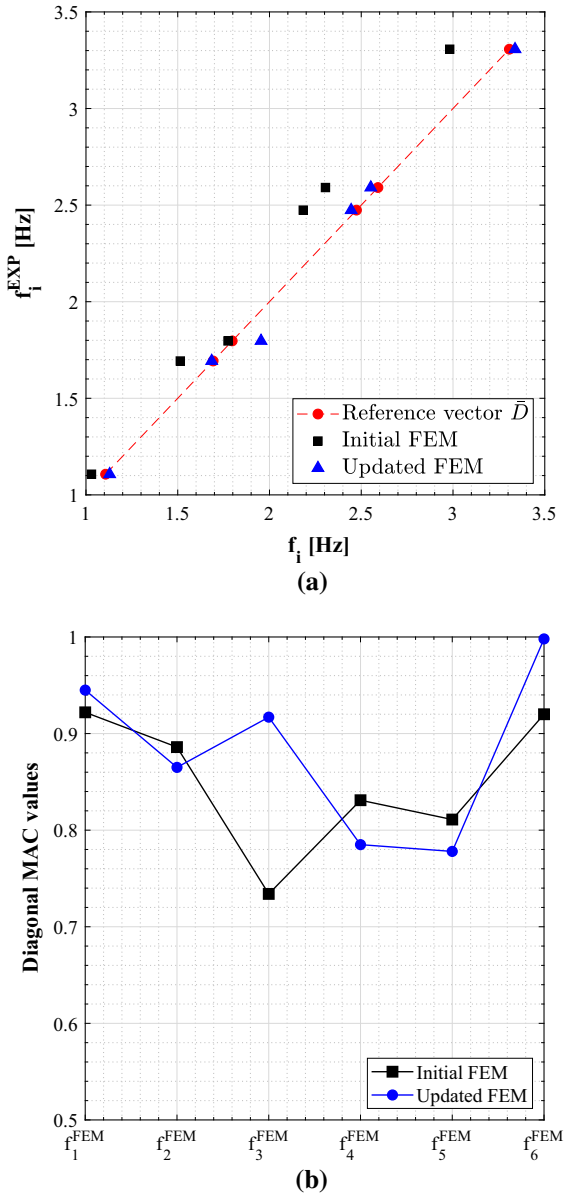

Fig. 12 FEM responses before and after the updating Bayesian procedure: **a** natural frequencies; **b** diagonal MAC values

(Umbria Region, Central Italy). The obtained results demonstrated the importance of using suitable informative data sets. In this case study it was found that the natural frequencies were mainly influenced by the deck stiffness rather than the cable stiffness. Work is in progress to investigate the effect of changes in the updating parameters on the numerical model mode shapes variations in order to improve the likelihood function in the Bayesian updating framework, obtaining a more informative experimental data set.

Compliance with ethical standards

Conflict of interest The authors declare that they have no conflict of interest.

References

1. Allemang AJ (2003) The modal assurance criterion (MAC): twenty years of use and abuse. J Sound Vib 37:14–21
2. Au SK, Zhang FL, Ni YC (2013) Bayesian operational modal analysis: theory, computation, practice. Comput Struct 126:3–14. https://doi.org/10.1016/j.compstruc.2012.12.015
3. Bartoli G, Betti M, Facchini L, Marra A, Monchetti S (2017) Bayesian model updating of historic masonry towers through dynamic experimental data. Procedia Eng 199:1258–1263. https://doi.org/10.1016/j.proeng.2017.09.267
4. Bayes T (1763) An essay towards solving a problem in the doctrine of chances. Philos Trans R Soc 53:370–418
5. Beck JL (2010) Bayesian system identification based on probability logic. Struct Control Health Monit 17(7):825–847. https://doi.org/10.1002/stc.424
6. Beck JL, Katafygiotis LS (1998) Updating models and their uncertainties. I: Bayesian statistical framework. J Eng Mech 124(4):455–461 10.1061/(ASCE)0733-9399(1998)124:4(455)
7. Benedettini F, Gentile C (2011) Operational modal testing and fe model tuning of a cable-stayed bridge. Eng Struct 33(6):2063–2073. https://doi.org/10.1016/j.engstruct.2011.02.046
8. Bernardini E, Spence S, Gioffré M (2012) Dynamic response estimation of tall buildings with 3D modes: a probabilistic approach to the high frequency force balance method. J Wind Eng Ind Aerodyn 104–106:56–64. https://doi.org/10.1016/j.jweia.2012.03.014
9. Blatman G, Sudret B (2010) An adaptive algorithm to build up sparse polynomial chaos expansions for stochastic finite element analysis. Probab Eng Mech 25:183–197. https://doi.org/10.1016/j.probengmech.2009.10.003
10. Brincker R, Ventura C, Andersen P (2001) Damping estimation by frequency domain decomposition
11. Brincker R, Ventura CE (2015) Introduction to operational modal analysis. Wiley, Hoboken
12. Brincker R, Zhang L, Andersen P (2000) Modal identification from ambient responses using frequency domain decomposition. In: Proceedings of the international modal analysis conference—IMAC 1
13. Brownjohn JMW, Xia PQ (2000) Dynamic assessment of curved cable-stayed bridge by model updating. J Struct Eng 126(2):252–260. https://doi.org/10.1061/(ASCE)0733-9445(2000)126:2(252)
14. Choi SK, Canfield R, Grandhi R, Pettit C (2004) Polynomial chaos expansion with latin hypercube sampling for

estimating response variability. AIAA J 42:1191–1198. https://doi.org/10.2514/1.2220
15. Daniell WE, Macdonald J (2007) Improved finite element modelling of a cable-stayed bridge through systematic manual tuning. Eng Struct 29(3):358–371. https://doi.org/10.1016/j.engstruct.2006.05.003
16. Ewins D (1984) Modal testing: theory and practice. Mechanical engineering research studies: engineering dynamics series. Research Studies Press, Letchworth
17. Field R, Grigoriu M (2004) On the accuracy of the polynomial chaos approximation. Probab Eng Mech 19(1):65–80. https://doi.org/10.1016/j.probengmech.2003.11.017
18. Fleming J, Engin AE (1980) Dynamic behaviour of a cable-stayed bridge. Earthq Eng Struct Dyn 8(1):1–16. https://doi.org/10.1002/eqe.4290080102
19. Gamerman D, Lopes H (2015) Markov Chain Monte Carlo: stochastic simulation for Bayesian inference. Chapmann & Hall, CRC, Boca Raton
20. Ghaffar AMA, Khalifa MA (1991) Importance of cable vibration in dynamics of cable stayed bridges. J Eng Mech 117(11):2571–2589. https://doi.org/10.1061/(ASCE)0733-9399(1991)117:11(2571)
21. Ghanem R, Spanos P (1991) Stochastic finite elements: a spectral approach. Am J Math 60:897–936
22. Gioffré M, Gusella V (2007) Peak response of a nonlinear beam. J Eng Mech 133(9):963–969. https://doi.org/10.1061/(ASCE)0733-9399(2007)133:9(963)
23. Gioffré M, Gusella V, Cluni F (2008) Performance evaluation of monumental bridges: testing and monitoring 'Ponte delle Torri' in Spoleto. Struct Infrastruct Eng 4(2):95–106. https://doi.org/10.1080/15732470601155300
24. Hastings W (1970) Monte Carlo sampling methods using Markov chains and their applications. Biometrika trust, vol 57. Oxford University Press, Oxford
25. Jaynes ET (1957) Information theory and statistical mechanics. Phys Rev 106:620–630. https://doi.org/10.1103/PhysRev.106.620
26. Konakli K, Sudret B (2016) Polynomial meta-models with canonical low-rank approximations: numerical insights and comparison to sparse polynomial chaos expansions. J Comput Phys 321:1144–1169. https://doi.org/10.1016/j.jcp.2016.06.005
27. Marwala T (2010) Finite-element-model updating using computional intelligence techniques. Springer, London
28. Matthies HG (2007) Uncertainty quantification with stochastic finite elements. Encycl Comput Mech. https://doi.org/10.1002/0470091355.ecm071
29. McKelvey TP, Van Overschee P, De Moor B (1998) Book review: subspace identification for linear systems: theory, implementation, applications. Int J Adapt Control Signal Process 12(6):540–541. https://doi.org/10.1002/(SICI)1099-1115(199809)12:6<540::AID-ACS505>3.0.CO;2-L
30. Neal RM (2011) MCMC using Hamiltonian dynamics. Handbook of Markov Chain Monte Carlo
31. Peeters B, De Roeck G (1999) Reference-based stochastic subspace identification for output-only modal analysis. Mech Syst Signal Process 13:855–878
32. Pepi C, Gioffré M, Comanducci G, Cavalagli N, Bonaca A, Ubertini F (2017) Dynamic characterization of a severely damaged historic masonry bridge. Procedia Eng 199:3398–3403. https://doi.org/10.1016/j.proeng.2017.09.579
33. Rossi G, Marsili R, Gusella V, Gioffrè M (2002) Comparison between accelerometer and laser vibrometer to measure traffic excited vibrations on bridges. Shock Vib 9(1–2):11–18. https://doi.org/10.1155/2002/968509
34. Sap2000 (2018) Static and dynamic finite element of structures. Computers and Structures Inc, Berkeley
35. Saltelli A, Chan K (2000) Sensitivity analysis. Wiley, New York
36. Simoen E, De Roeck G, Lombaert G (2011) Resolution and uncertainty analysis of Bayesian FE model updating results. In: Proceedings of the 8th international conference on structural dynamics, EURODYN 2011, pp 2318–2325
37. Simoen E, Roeck GD, Lombaert G (2015) Dealing with uncertainty in model updating for damage assessment: a review. Mech Syst Signal Process 56–57:123–149. https://doi.org/10.1016/j.ymssp.2014.11.001
38. Sobol I (1993) Sensitivity estimates for non linear mathematical model. Math Comput Simul 1:56–61
39. Sobol I (2001) Global sensitivity indices for nonlinear mathematical models and their Monte Carlo estimates. Math Comput Simul 55(1):271–280. https://doi.org/10.1016/S0378-4754(00)00270-6
40. Sudret B (2008) Global sensitivity analysis using polynomial chaos expansions. Reliab Eng Syst Saf 93(7):964–979. https://doi.org/10.1016/j.ress.2007.04.002
41. Sudret B, Marelli S, Wiart J (2017) Surrogate models for uncertainty quantification: an overview. In: 2017 11th European conference on antennas and propagation (EUCAP), pp 793–797
42. Tarantola A (2005) Inverse problem theory and methods for model parameter estimation. Soc Ind Appl Math. https://doi.org/10.1137/1.9780898717921
43. Ren WX, Peng XL, Lin YQ (2005) Experimental and analytical studies on dynamic characteristics of a large span cable-stayed bridge. Eng Struct 27(4):535–548. https://doi.org/10.1016/j.engstruct.2004.11.013
44. Wiener N (1938) The homogeneous chaos. Am J Math 60:897–936
45. Xiu D, Karniadakis GE (2002) The Wiener–Askey polynomial chaos for stochastic differential equations. SIAM J Sci Comput 24(2):619–644
46. Yuen KV, Beck JL, Katafygiotis SL (2001) Efficient model updating and health monitoring methodology using incomplete modal data without mode matching. Struct Control Health Monit 13(1):91–107. https://doi.org/10.1002/stc.144